Master's Thesis

Engineering *Escherichia coli* to Exploit Alternative Glycolytic Pathways upon Complete Loss of the Upper Embden-Meyerhof-Parnas Pathway

Ye Eun Kim

Department of Chemical Engineering

Graduate School of UNIST

2019

Engineering *Escherichia coli* to Exploit Alternative Glycolytic Pathways upon Complete Loss of the Upper Embden-Meyerhof-Parnas Pathway

Ye Eun Kim

Department of Chemical Engineering

Graduate School of UNIST

Engineering *Escherichia coli* to Exploit Alternative Glycolytic Pathways upon Complete Loss of the Upper Embden-Meyerhof-Parnas Pathway

A thesis/dissertation

submitted to the Graduate School of UNIST

in partial fulfillment of the

requirements for the degree of

Master of Science

Ye Eun Kim

07/05/2019

Approved by

_____

Advisor

Sung Kuk Lee

Engineering *Escherichia coli* to Exploit Alternative Glycolytic Pathways upon Complete Loss of the Upper Embden-Meyerhof-Parnas Pathway

Ye Eun Kim

This certifies that the thesis/dissertation of Ye Eun Kim is approved.

07/05/2019

signature

_____

Advisor: Sung Kuk Lee

signature

_____

Sung Hoon Park: Thesis Committee Member #1

signature

_____

Yong Hwan Kim: Thesis Committee Member #2

Abstract

The glycolytic pathway has a central role in metabolism by supplying precursor, energy and redox molecules for supporting well-being of microorganism at natural habitat. Advent of synthetic biology, however, facilitates proliferation of microorganisms beyond their original niche. The native glycolytic pathway often contains thermodynamic bottleneck and stoichiometry limiting their wide-range application. Adopting alternative glycolytic structure bypassing such metabolic hurdles enables to expand and diversify traits of a microbial strain. Here, we completely inactivate the Embden-Meyerhof-Parnas (EMP) pathway in *Escherichia coli* which functions as major glycolytic route. In order to surpass sub-optimality of latent alternative glycolytic routes in glucose catabolism, *E. coli* strain without the functional EMP pathway was subjected to adaptive evolution with glucose as sole carbon source. The evolved mutant exhibiting 6.6-fold higher growth rate was isolated. Based on whole genome sequencing data, key genotype changes were identified from genotype-phenotype relationship. Disabilities of glucose uptake and glucose catabolism sole *via* the Pentose-phosphate (PP) pathway were identified as primary metabolic bottlenecks upon complete loss of the upper EMP pathway. These can be resolved by simultaneous enabling of glucose uptake and activating latent the Entner-Doudoroff (ED) pathway for glucose catabolism. By rebalancing two alternative glycolytic pathways, the ED and PP pathway, tuning profile of carbon, energy and redox equivalents yield from glucose was demonstrated. Combining the rebalancing strategy to adaptive evolution, 3-hydroxypropionic acid (3-HP) production titer was increased up to 3.2-fold compared to the unevolved strain.

Contents

List of figures

List of tables

Nomenclature

E. coli: *Echerichia coli*

Z. mobilis: *Zymomonas mobilis*

C. aurantiacus: *Chloroflexus aurantiacus*

EDA50: 50-Day adapted Δ*pfkAB* strain

EMP: Embden-Meyerhof-Parnas

PP: Pentose phosphate

ED: Entner-Doudoroff

ALE: Adaptive Laboratory Evolution

OD: Optical density

LB: Luria-Bertani

SOC: Super optimal catabolite repression

IPTG: Isopropyl β-D-1-thiogalactopyranoside

DNA: Deoxyribonucleic acid

PCR: Polymerase chain reaction

FRT: Flippase recognition target

FLP: Flippase

RFP: Red fluorescent protein

HPLC: High-performance liquid chromatography

PFK: Phosphofructokinase

G6PDH: glucose 6-phosphate dehydrogenase

PTS: Phosphotransferase system

3-HP: 3-Hydoryxpropionic acid

MCR: Malonyl-CoA reductase

ACC: Acetyl-CoA carboxyltransferase

GLC: Glucose

G6P: Glucose 6-phosphate

F6P: Fructose 6-phsophate

FBP: Fructose 1,6-bisphosphate

DHAP: Dihydroxyacetone phosphate

GAP: Glyceraldehyde 3-phosphate

1,3-BGP: 1,3-Bisphosphoglycerate

G3P: Glycerate 3-phosphate

PEP: Phosphoenolpyruvate

PYR: Pyruvate

PGL: 6-Phosphogluconolactone

6PG: 6-Phosphogluconate

Ru5P: Ribulose 5-phosphate

R5P: Ribose 5-phosphate

X5P: Xseylose 5-phosphate

S7P: Sedoheptulose 7-phosphate

E4P: Erythrose 4-phosphate

KDPG: 2-dehydro-3-deoxy-phosphogluconate

ATP: Adenosine triphosphate

ADP: Adenosine diphosphate

NAD(H): Nicotinamide adenine dinucleotide

NADP(H): Nicotinamide adenine dinucleotide phosphate

**cAMP:** Cyclic adenosine monophosphate

I. Introduction

Across the domains of life the glycolytic pathway is a shared carbon feeding module catabolizing monosaccharaides into pyruvate and energy [1-3]. The Embden-Meyerhof-Parnas (EMP) pathway is a typical sequence of the glycolytic pathway [4]. *Escherichia coli* also metabolize a glucose *via* the EMP pathway and generate two pyruvates as well as two NADH and two ATP [5].

Parallel with increasing attention on value-added chemical production in microbial cell factories, necessity of developing microbial host for enhanced bioconversion efficiency has raised [6]. Considering primary role of glycolysis in serving energy, reducing equivalents and precursors for synthesis of small molecules and cell skeleton, engineering to facile and versatile structure is highly desirable [7].

Despite of prevalence as glycolysis, the EMP pathway possesses two thermodynamic bottlenecks at fructose 6-phosphate aldolase and triose-phosphate isomerase [8]. In addition, phosphofructokinase catalyzing one of the committed steps in the EMP pathway is subjected to intensive regulations on transcription, translation, and even post-translation and allosteric level by distal metabolites such as PEP and citrate as well as energetic precursor such as AMP, ADP, and ATP [9]. Regeneration rate of redox equivalent in the EMP pathway is under the anabolic demand [10].

Responding to challenges of diverse and dynamic local niches, some of microorganism have adapted alternative glycolytic pathway such as the Entner-Doudoroff (ED) or Pentose Phosphate (PP) pathway[11]. They are all distinct in terms of thermodynamic and metabolite profile [12]. Compared to the EMP pathway, the ED pathway generates one less ATP during conversion of glucose-6-phsophate to pyruvate [12]. Thermodynamic analysis of the ED pathway showed that at the expense of missing one ATP generation it can carry the same metabolic flux with 3.5-fold less enzyme compared to the EMP pathway [8, 13]. In addition, *Zymomonas mobilis* exclusively relying on the ED pathway shows remarkably fast glucose uptake and ethanol production rate [14]. When the PP pathway runs as major glycolytic pathway upon absence of phosphofructokinase, it operates in partially cyclized manner regenerating extreme amount of NADPH. In the unique metabolic architecture called the partial cyclic PP pathway transketolase or transaldolase produces fructose 6-phosphate, which is in turn converted into glucose 6-phsohate again *via* reverse reaction of phosphoglucose isomerase. Then it can enter PPP again. Upon complete recycling of fructose 6-phosphate of 6 molecules of NADPH can be be regenerated per a molecule of glucose [15].

Figure 1. The major and alternative glycolytic pathways in *Escherichia coli*. (a) The central carbon metabolism in *E. coli*. The Embdem-Meyerhof-Parnas (EMP), the Pentose Phosphate (PP), and the Entner-Doudoroff (ED) pathway are shown in blue, orange and green, respectively. Schematic representation of native glycolytic flux (b) to the redirected glycolytic routes upon elimination of phosphofructokinase (c). Dots, squares, and triangles indicate metabolites, redox and energy equivalents, respectively.
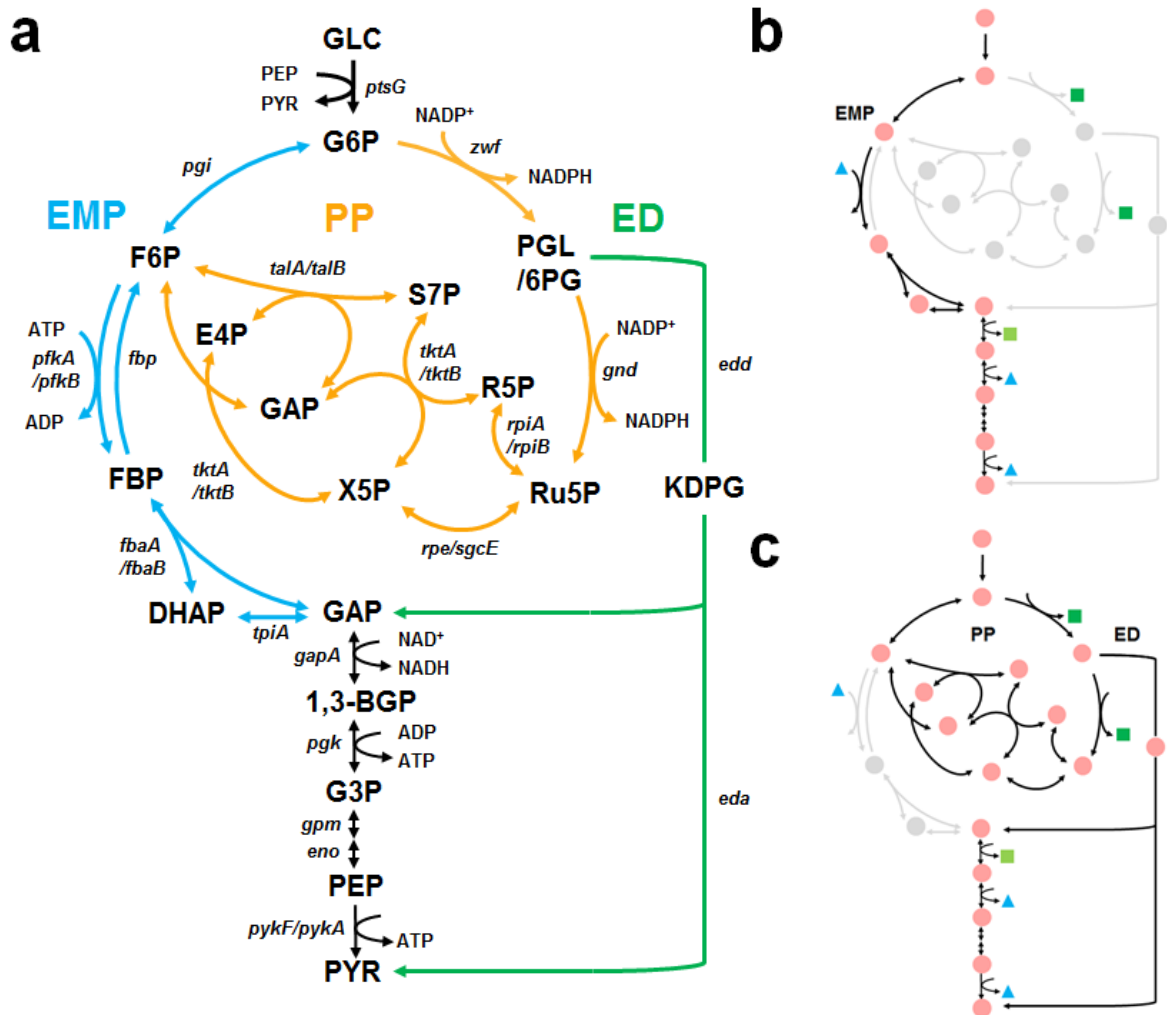
In *E. coli*, it was demonstrated that disruption of the EMP pathway at the phosphofructokinase or phosphoglucose isomerase redirected glycolytic flux to the ED or PP pathway [16]. However, these mutants showed retarded glucose uptake rate and biomass accumulation during growth on glucose as a major carbon source due to un-optimized alternative route [16]. So far studies on physiology of mutants with reduced phosphofructokinase activity was reported [16-19], which was followed by efforts to engineer such mutants to address those issues based on the discoveries. However, limited information due to the unusual features of the metabolism hampers successful rational design of

12

II. Materials and methods

2.1 Bacterial strains, plasmids and general techniques

The bacterial strains and plasmids used in this study are listed in Table 1. Wild type *E. coli* MG1655 strain was used as parent strains to construct mutant strains.

For plasmid isolation, LaboPass plasmid miniprep kit (Cosmo Genentech, Korea) was used. DNA purification (103-102) and gel extraction kits (102-102) were purchased from GeneAll Biotechnology (Seoul, Korea). The primers were synthesized by Macrogen Inc. (Seoul, Korea). Unless indicated, chemicals were purchased from Sigma-Aldrich (St. Louis, MO, USA).

Antibiotics were used as following concentrations: ampicillin (100 mg/ml), kanamycin (50 mg/ml) or chloramphenicol (30 mg/ ml).

Table 1. Strains and plasmids used in this study.

Strains/plasmids	Genotype and description	Source
Strains		
MG1655	*E. coli* K-12 F^- λ^- *ilvG*$^-$ *rfb-50 rph-1*	[24]
$\Delta pfkA$	MG1655 $\Delta pfkA$::FRT	[25]
$\Delta pfkAB$	$\Delta pfkA$ $\Delta pfkB$::FRT	[25]
Δpgi	MG1655 Δpgi::FRT	[25]
EDA50	$\Delta pfkAB$ adapted in glucose minimal media	[25]
EDA50-2	$\Delta pfkAB$ adapted in glucose minimal media	[25]
EDA50-3	$\Delta pfkAB$ adapted in glucose minimal media	[25]
EDA50-4	$\Delta pfkAB$ adapted in glucose minimal media	[25]
EDA50-5	$\Delta pfkAB$ adapted in glucose minimal media	[25]
EDA50_n	EDA50 $\Delta gntR^{A141E}$::$gntR^{wt}$ (*a*422c)	This study
EDA50_l	EDA50 $\Delta galR^{G271D}$::$galR^{wt}$ (*a*812g)	This study
EDA50_u	EDA50 (ugd-gnd-wbbL-2)$^+$ (2312bp deletion in ugd-gnd-wbbL-2 was replaced by the wild type allele)	This study
EDA50_c	EDA50 Δcrp^{A85S}::crp^{wt} (t253g)	This study
EDA50_t	EDA50 $\Delta talB^{A247V}$::$talB^{wt}$ (t740c)	This study
AB_n	$\Delta pfkAB$ $\Delta gntR$::$gntR^{A141E}$ (c422a)	This study
AB_l	$\Delta pfkAB$ $\Delta galR$::$galR^{G271D}$ (g812a)	This study
AB_u	$\Delta pfkAB$ $\Delta(ugd\text{-}gnd\text{-}wbbL\text{-}2)$::FRT	This study
AB_lu	AB_l $\Delta(ugd\text{-}gnd\text{-}wbbL\text{-}2)$::FRT	This study
AB_nu	AB_n $\Delta(ugd\text{-}gnd\text{-}wbbL\text{-}2)$::FRT	This study
AB_nl	AB_n $\Delta galR$::$galR^{G271D}$ (g812a)	This study

AB_nul	AB_nu $\Delta galR::galR^{G271D}$ (g812a)	This study
AB_nulc	AB_nul $\Delta crp::crp^{A85S}$ (g253t)	This study
EDA50_Δn	EDA50 $\Delta gntR^{A141E}::FRT$	This study
EDA50_n pGalP	EDA50_n with pGalP	This study
EDA50_Δl	EDA50 $\Delta galR^{G271D}::FRT$	This study
EDA50_l pEdd-Eda	EDA50_l with pEdd-Eda	This study
EDA50_u Δgnd	EDA50_u $\Delta gnd::FRT$	This study
EDA50 pRFP	EDA50 with pRFP	This study
EDA50 pGnd	EDA50 with pGnd	This study
EDA50 pGnd-GntR	EDA50 with pGnd-GntR	This study
MG1655 fabI^{ts}	MG1655 ΔfabI::fabI^{S241F}_FRT	This study
$\Delta pfkA$ fabI^{ts}	$\Delta pfkA$ ΔfabI::fabI^{S241F}_FRT	This study
$\Delta pfkAB$ fabI^{ts}	$\Delta pfkAB$ ΔfabI::fabI^{S241F}_FRT	This study
Δpgi fabI^{ts}	Δpgi ΔfabI::fabI^{S241F}_FRT	This study
EDA50 fabI^{ts}	EDA50 ΔfabI::fabI^{S241F}_FRT	This study
MG1655 fabI^{ts} pMCR pACC	MG1655 ΔfabI::fabI^{S241F}_FRT pMCR pACC	This study
$\Delta pfkA$ fabI^{ts} pMCR pACC	$\Delta pfkA$ ΔfabI::fabI^{S241F}_FRT pMCR pACC	This study
$\Delta pfkAB$ fabI^{ts} pMCR pACC	$\Delta pfkAB$ ΔfabI::fabI^{S241F}_FRT pMCR pACC	This study
Δpgi fabI^{ts} pMCR pACC	Δpgi ΔfabI::fabI^{S241F}_FRT pMCR pACC	This study
EDA50 fabI^{ts} pMCR pACC	EDA50 ΔfabI::fabI^{S241F}_FRT pMCR pACC	This study
EDA50 pGnd fabI^{ts} pMCR pACC	EDA50 ΔfabI::fabI^{S241F}_FRT pGnd pMCR pACC	This study
EDA50 pGnd-GntR fabI^{ts} pMCR pACC	EDA50 ΔfabI::fabI^{S241F}_FRT pGnd-GntR pMCR pACC	This study
MG-LacZ40a	MG $\Delta lacZ_{838-879}::P_{P3BCD2}$-tetA	[26]

Plasmids

pBbS6a-rfp	SC101 *ori*, carrying $P_{LlacO-1}$ promoter and rfp, Amp^R	[27]
pBbE2k-rfp	ColE1 *ori*, carrying P_{tetO} promoter and rfp, Kan^R	[27]
pBbA6c-rfp	pA15 *ori*, carrying $P_{LlacO-1}$ promoter and rfp, Cm^R	[27]
pGalP	pBbS6a with $\Delta rfp::galP$ (from MG1655), Amp^R	This study
pEdd-Eda	pBbS6a with $\Delta rfp::edd\text{-}eda$ (from MG1655), Amp^R	This study
pRFP	pBbS5a-rfp; SC101 *ori*, P_{lacUV5} promoter and rfp, Amp^R	[27]
pGnd	pRFP with $\Delta rfp::gnd$ (from MG1655), Amp^R	This study
pGnd-GntR	pRFP with $\Delta rfp::gnd\text{-}gntR$ (from MG1655), Amp^R	This study
pSIM5	SC101-ts *ori*, carrying heat-shock inducible λ-RED recombinase system, Cm^R	[28]

pKD13	Template for kanamycin cassette flanked by FRT sites, Km[R]	[29]
pCP20	SC101-ts *ori*, carrying constitutively expressed yeast FLP recombinase, Am[R],Cm[R]	[30]
pCDF-mcrC*-mcrN	pCDF-*mcrC**(N391V/K557W/S565N) –*mcrN*	[31]
pMCR	pBbE2k-*mcrC**(N391V/K557W/S565N) –*mcrN*	This study
pBbA2k-accDABC	pBbA2k-rfp with Δ*rfp*::*accD*, *accA*, *accB* and *accC*, Km[R]	[32]
pACC	pBbA6c-*rfp* with Δ*rfp*::*accD*, *accA*, *accB* and *accC*, Km[R]	This study

2.2 Adaptive Laboratory evolution

In order to isolate fast-growing mutant even without the functional EMP pathway, the mutant with both *pfkA* and *pfkB* genes deleted was adapted by serially transfer method in previous study [25]. Briefly, overnight grown Δ*pfkAB* mutant in LB was transferred to M9 minima media (BioShop Canada Inc., Burlington, Canada) supplemented with 2 mM $MgSO_4$, 0.1 mM $CaCl_2$ and 5 g/L glucose and grown in 37 °C and 200 rpm. At optical density at 600 nm (OD_{600}) around 1.0, cells were passed to fresh media. This procedure was repeated during 50 times. Then, 50th-time subultured cells were plated on to LB agar plate. Five evolved mutant showing the fastest biomass accumulation were screened by OD_{600} monitored by 96-well microplate reader (Infinite M200 TECAN, Austria) and named as EDA50, EDA50-2 to -5.

2.3 Genome sequencing

Whole genome sequencing of EDA50 was conducted as mentioned before. [25] Briefly, genomic DNA of EDA50 was isolated by using DNA isolation kit (GeneAll Biotechnology Co., Korea). It was sequenced by Next Generation Sequencing using Illumintha HiSeq 2000 sequencer (Macrogen Inc., Korea). The genomic sequence of *E. coli* MG1655 (NC_000913.3) was used as reference.

Occurrence of mutations was confirmed by DNA sequencing of PCR amplicon of target region in the unevolved and evolved mutant. In order to analyze mutation frequency, for four other EDA50 mutants existence of either the same or equivalent to mutation discovered in EDA50 was analyzed by PCR amplification and DNA sequencing.

2.4 Genetic manipulation

Plasmids were transformed by preparation of electrocompetent cells and electric impulse [33]. Overnight grown cells were 1:100 diluted to fresh media. After grown until OD_{600} around 0.5, Cells were harvested (13200 g, 1 min, 4 ℃) and washed three-times with ice-cold distilled water. After cells were

re-suspended with 50 µL ice-cold distilled water, approximately 100 ng of the plasmid were added and transformed by electroporation using a MicroPulser (BioRad, Hercules, CA). Then, the electric-shocked cells were incubated in 1 mL SOC for 3 hours and plated on to LB agar plate with appropriate antibiotics for selection. Cells carrying plasmid with temperature-sensitive origin were grown at 30 ℃ for plasmid maintenance. Otherwise, cells were grown at 37 ℃.

To construct knock-out mutant, homologous recombination based on λ RED recombination system was used, which was mediated by kanamycin resistance (Km^R) cassette flanked by FLP recognition target (FRT) knock-in and flippase-based curing [30]. Knock-in FRT-flanked Km^R cassettes were obtained by PCR amplification using primers designed to amplify FRT-Km^R-FRT region from pKD13 with 50 bp overhang homologous to targeted deletion site. All cassettes were amplified using Pfu-X DNA Polymerase (Solgent, Seoul, Korea). First, the helper plasmid pSIM5 carrying λ RED recombination system was transformed. The resulting cells were rendered to be electrocompetenet by the above-mentioned procedure with an addition of a step where just before being harvested cells were heat-shocked at 42 ℃ for 15 minutes to induce the λ RED system One-step inactivation of chromosomal genes in Escherichia coli K-12 using PCR products [29]. After transformation of the knock-in cassette and selection on LB agar plate with appropriate antibiotics, correct integration was confirmed using colony PCR. The knocked-in Km^R gene was cured by transformation of flippase-carrying pCP20. Then cells were streaked on LB agar plate with no antibiotics and grown overnight at 42 ℃ to dilute out temperature-sensitive pSIM5 and pCP20. Cells were screened for antibiotics sensitivity and for those without any antibiotics resistance removal of the Km^R gene was confirmed by colony PCR and sequencing.

For construction of single-mutation-repaired EDA50 or mutation introduced Δ*pfkAB* mutant, λ RED recombination system together with tetA cassette enabling tetracycline-based dual selection system was used [26]. tetA cassettes were prepared by PCR amplification using primers p3-BCD2-tetA region from MG-LacZ40a with 50 bp overhang homologous to designated insertion site. For transformation of the tetA cassette, cells were prepared following the procedure for transformation of Km^R cassette during gene deletion. After electric shock cells were recovered at 30 ℃. At the same temperature, selection was conducted in presence of chloramphenicol together with tetracycline to maintain pSIM for following transformation. The wild-type or mutant allele fragments replacing the inserted tetA cassette were prepared by PCR amplification using MG1655 or EDA50 as template with 50 bp overhang homologous to designated insertion site. Again, cells were transformed with replacing DNA fragment by the early method. After recovery, cells still possessing tetA cassette cells were ruled out and true transformants were enriched by the previous method with minor modification [26]. Briefly, the transformed cells were 100-fold diluted to liquid 0.5% glucose M9 medium supplemented with 2 mM MgSO$_4$, 0.1 mM CaCl$_2$ and 50 µM of NiCl$_2$ and grown over-night. Then, approximately 10^2 to

10^3 cells were spread onto antibiotics-free LB agar plate and grown at 42 ℃. After screened for antibiotics sensitivity and for those without any antibiotics resistance correct allelic replacement was confirmed by colony PCR and sequencing.

2.5 Plasmid construction

  All plasmids constructed here were derived from BioBrick plasmids [27]. To construct pBbA6c-*edd-eda*, the gene encoding red fluorescent protein (RFP) in the pBbA6c-*rfp* vector was digestion with EcoRI and BamHI. The *edd-eda* gene cluster was amplified from *E. coli* MG1655 genomic DNA with a forward primer containing an EcoRI site and a reverse primer containing a BamHI sites. Purified *edd-eda* fragment after digested with EcoRI and BamHI was ligated with the gel-eluted pBbA6c backbone.

  For cloning *galP* gene, the gene encoding RFP in the pBbS6k-*rfp* vector was digestion with BglII and XhoI. The *E. coli galP* gene was amplified from *E. coli* MG1655 genomic DNA with a forward primer containing a BglII site and a reverse primer containing a XhoI sites. Purified *galP* fragment after digested with BglII and XhoI was ligated with the gel-eluted pBbS6k backbone.

  In order to construct pBbS5a-*gnd*, the gene encoding RFP in the pBbS5a-rfp vector was digestion with EcoRI and XhoI. The *E. coli gnd* gene was amplified from *E. coli* MG1655 genomic DNA with a forward primer containing an EcoRI site and a reverse primer containing XhoI sites. Purified *gnd* fragment after digested with EcoRI and XhoI was ligated with the gel-eluted pBbS6k backbone.

  For construction of pBbS5a-*gnd-gntR,* the *E. coli gntR* gene was amplified from *E. coli* MG1655 genomic DNA with a forward primer containing a BglII site and a reverse primer containing XhoI sites. Purified *gntR* fragment after digested with BglII and XhoI was ligated with the purified pBbS6k-gnd after digestion with BamHI and XhoI.

  For constructing pMCR plasmid, mcrC*-mcrN fragment including genes encoding dissected C-terminal domain carrying three mutation (N391V/K557W/S565N) and N-terminal domain of malonyl-CoA reductase from *Chloroflexus aurantiacus* was extracted after digesting pCDF- mcrC*-mcrN plasmid at EcoRI and XhoI site [31]. The pBbE2k-rfp plasmid was digested with EcoRI and XhoI for removal of gene encoding RFP. The DNA fragment and the gel-eluted pBbE2k backbone were ligated. For construction of pACC plasmid, fragment of accDABC gene cluster encoding acetyl-CoA acetyl-CoA carboxyltransferase (ACC) complex was obtained from elution after digesting pBbA2k-accDABC at BglII and XhoI site. The pBbA6c-rfp plasmid was digested with BglII and XhoI for removal of gene encoding RFP. After gel-elution, pBbA6c backbone was ligated with the eluted accDABC fragment.

  All cloned genes were amplified by using Pfu-X DNA Polymerase and all restriction enzymes used

were purchased from Fermentas (Vilnius, Lithuania). Primers used for plasmid cloning were listed in Table 2.

Table 2. Primers used in this study.

Primer	Sequence (5'-3')
gntR_H1_P1	GTCCGTGTTAAACTAAGAGAATCTATCTCTTTTGTACCTTCAGGACGATGGTGTAGGCTGGAGCTGCTTC
gntR_H2_P4	CCATGCCTTAAGTGTATAAGTGTGAGCTACTTCAAATTTGTGGGCTTAAAATTCCGGGGATCCGTCGACC
gntR_seqFP	GCCTTTTTGCAGGCTTCCTC
gntR_seqRP	CCCGATACGCCCATCAAGAC
galR-tetA_P1	CGTTCTCAATGATAATGGTATTGATGTACCGGGTGAGATTTCGTTAATTGGTGTAGGCTGGAGCTGCTTCG
galR_H2_P4	CAGACCATCGAAGAATTACTGGCGCTGGAATTGCTTTAACTGCGGTTAGTATTCCGGGGATCCGTCGACC
galR-FP	TAATGAAACAAATGCCCGGT
galR-RP	TGCCGGAAGTGAAGGCAGGT
galR_seqFP	GGCTCACATTCCCACGATG
galR_seqRP	GGGCGATGTCTTTACCCAG
ugd-gnd-wbbL delFP	TAATCAGCATCCCGGTAGGCTTCATTTTTATCTAATGTGGCATTAAAGTGATTCCGGGGATCCGTCGACC
ugd-gnd-wbbL delRP	GAAATGACTGAGTCAGCCGAGAAGAATTTCCCCGCTTATTCGCACCTTCCGTGTAGGCTGGAGCTGCTTCG
ugd-gnd-wbbL FP	TAATCAGCATCCCGGTAGGC
ugd-gnd-wbbL RP	GAAATGACTGAGTCAGCCGAG
wbbL_2 insFP	TTATTAAAGTATAAATAGCTTATCCATGCTTATATGCTTACGGCTTTATAGTGTAGGCTGGAGCTGCTTC
wbbL_2 insRP	TTTTATCAAATCGCAACTTTGATCGAATTTCATCAGTTTTTCACCCGTAAATTCCGGGGATCCGTCGACC
wbbL_2_kanR	GTGTATACCTTATCTGCCACATCCTTAAGCTCTTCTGCCATTCGG
zzB_insFP	TTAGAGATAATGACGTCGGTTCATGCTCTCAGAATTAACTTAAC
ugd seqRP	CATCATTACCCTAACTGACGG
crp_H1_P4	GGCGTTATCTGGCTCTGGAGAAAGCTTATAACAGAGGATAACCGCGCATGATTCCGGGGATCCGTCGACC
crp_H2_P1	CTACCAGGTAACGCGCCACTCCGACGGGATTAACGAGTGCCGTAAACGACGTGTAGGCTGGAGCTGCTTCG
crp-FP	TTGATGTACTGCATGTATGC
crp-RP	ATGGCGCGCTACCAGGTAAC
crp_seqFP	ATAGCCCCTTCCCAGGTAG
crp_seqRP	CAGGAACGAGGGAGAAGAG
talB_H1_P1	AGACCGGTTACATCCCCCTAACAAGCTGTTTAAAGAGAAATACTATCATGGTGTAGGCTGGAGCTGCTTC
talB_H2_P4	CTTCAGAAGAGGTAGCGTGACCGACTTCCCGGTCACGCTAAGAATGATTACAATTCCGGGGATCCGTCGACC
talB-FP	AAAGCAAAACGCCTGATCAA
talB-RP	GCGCAGGGATGCCTTTATCC

19

talB_seqFP	CTGGCGATAACCGTCTTGTC
talB_seqRP	CCTGCTCATCGGGGATTAAG
EcoRI_RBS_eddEc FP	CCCCCGAATTCTGACAACTCAATTTCAGGAGCCTTTATGAATCCACAACTACTGCGCGTAACAAATCGAATCATTG
BamHI_edaEc RP	CCCGGATCCTTACAGCTTAGCGCCTTCTAC
BglII_RBS_galPEc FP	CCAGATCTAAAAATAACCATATTGGAGGGCATC
XhoI_galPEc RP	CCCCCTCGAGTTAATCGTGAGCGCCTATTTC
gnd_H1_P1	AGGCCGCGAGCATTCAGCGCGGTGATCACACCTGACAGGAGTATGTAATGGTGTAGGCTGGAGCTGCTTC
gnd_H2_P4	GTGCAATATACGCCGGGCCTCAATTTTATTGTTGGTTAAATCAGATTAATATTCCGGGGATCCGTCGACC
gnd seqFP_2	GATTTGATGACCATAACCGC
gnd seqRP_2	GTCAGTGGGAGAGATCTCAC
EcoRI-BglII-gnd FP	CCCCCCGAATTCAAAAGATCTTGATCACACCTGACAGGAGT
XhoI-BamHI gnd RP	GGGGGGCTCGAGTTTGGATCCTTAATCCAGCCATTCGGTATGG
EcoRI_BglII gntR FP	CCCCCCGAATTCAAAAGATCTCTGGACGGAAGTCCAGGCCATAAACATGAAAAAGAAAGACCCGTACTTC
XhoI-BamHI gntR RP	GGGGGGCTCGAGTTTGGATCCTTAAATAGATCCGCCCGGTG
fabI(S241F)_km SOE P1	TGTGGGTAACTCTGCGGCATTCCTGTGCTCCGATCTCTCTGCCGGTATCTTCGGTGAAGTGGTCCACGTTGACGGCGGTTTCAGCATTGCTGCAATGAACG
fabI(S241F)_km SOE P2	GGTCGACGGATCCCCGGAATTTATTTCAGTTCGAGTTCGTTCATT
fabI(S241F)_km SOE P3	AATGAACGAACTCGAACTGAAATAAATTCCGGGGATCCGTCGACC
fabI(S241F)_km SOE P4	AACAGAGATAACGGGCGGCAGAACGCCGCCCATCTTTACCAACAGAACGAGTGTAGGCTGGAGCTGCTTC
(Km)P4-fabIp_HR	TTAATTCTCATGTTTGACAGCCTGCTCCGGTCGGACCTGG
fabI seqRP	ACCTTTGCGGCTTCCGGGAC

2.6 Cell culture

For growth measurement, a single colony from an agar plate was inoculated in 3 mL of LB medium at 37 ℃ at 200 rpm. Overnight-grown cells were 1:10 transferred to 4 mL of the M9 medium supplemented with 2 mM $MgSO_4$, 0.1 mM $CaCl_2$ and 5 g/L glucose with appropriate antibiotics if required. After grown for 9 hours, cells were inoculated into 25 mL of the M9 medium in a 250-mL shaking flask at 37 ℃ at 200 rpm to achieve an initial OD_{600} around 0.1. Expression of *galP* and *edd-eda* was induced by the addition of 6.25 µM of IPTG at the beginning of both subculture and culture. Expressions of pRFP, pGnd and pGnd-GntR plasmids were induced by the addition of 50 µM of IPTG 3 h after culture start. OD_{600} was measured on a spectrophotometer (Libra S22).

For 3-HP production, a single colony from an agar plate was inoculated in 3 mL of LB medium at 37 ℃ at 200 rpm. Overnight-grown cells were 1:20 inoculated to M9 media supplemented with 20

g/L glucose, 1.0 g/L yeast extract, 2 mM $MgSO_4$, 0.1 mM $CaCl_2$ and trace elements. The composition of trace element solution is as follow: 2.4 g of $FeCl_3 \cdot 6H_2O$, 0.3 g of $CoCl_2 \cdot 6H_2O$, 0.15 g of $CuCl_2 \cdot 2H_2O$, 0.3 g of $ZnCl_2$, 0.3 g of $Na_2MO_4 \cdot 2H_2O$, 0.075 g of H_3BO_3, and 0.495 g of $MnCl_2 \cdot 4H_2O$ per liter [32]. After grown at 30 ℃ and 200 rpm for 9 hours, 50 µM of IPTG and 100 nM of tetracycline for expression of *mcrC*-mcrN* and *accDABC*. Just after inducers were added, temperature was increased to 37 ℃.

2.7 [NADPH]/[NADP$^+$] measurement

At 3-hour post-induction, Intracellular pyridine nucleotides $NADP^+$ and NADPH were extracted and assayed using EnzyChrom™ $NADP^+$/NADPH assay kit (BioAssay Systems, Hayward, CA, USA) following the manufacturer's instructions.

2.8 Analytical method

Concentrations of glucose and 3-HP were measured by HPLC using the method previously described with slight modification [34]. After 20-fold diluted, 20 µL of samples were injected into an a 300 mm × 7.8 mm Aminex HPX-87H (Bio-Rad, USA) column at 35 ℃ using 5.41 mM H_2SO_4 as mobile phase.

Culture media was treated using previously reported method with minor modifications [35]. After centrifuging for 30 minutes at 13,200 g, the supernatant was heat-treated at 80 ℃ for 1 hour. Then, the supernatant acquired after centrifuging again for 30 minutes at 13,200 g was used for analysis.

Ⅲ. Results

3.1 Adaptive evolution of phosphofructokinase-deficient *E. coli* mutant

  In *E. coli*, there are two phosphofructokinase (PFK) isozymes, PFK-1 and PFK-II encoded by *pfkA* and *pfkB*, respectively [36]. In order to construct mutant without functional EMP pathway, mutant with both *pfkA* and *pfkB* deleted was constructed. The double knock-out mutant exhibited virtually no growth with glucose as sole carbon source [16] (Fig. 2). In order to enable glucose utilization as sole carbon source and consequent growth, the Δ*pfkAB* mutant was adapted for 50-time subcultured in M9 minimal media with 5g/L glucose by sequentially transferring to fresh media at stationary phase. Mutant showing the fastest cell growth was isolated as denoted as EDA50. Fitness of the evolved mutant and the parental strain was estimated. Growth rate of the evolved mutant was significantly enhanced indicating that fast-growing mutant was successfully isolated from adaptive evolution experiment. The EDA50 exhibited 7.2-fold increased cell mass accumulation at 12-hour cultivation, which corresponds to 6.6-fold increased cell growth rate. Despite of discarded functional EMP pathway, it grew even faster than other mutants with partial blockage of the EMP pathway such as Δ*pfkA* and Δ*pgi* mutant did (Fig 2).
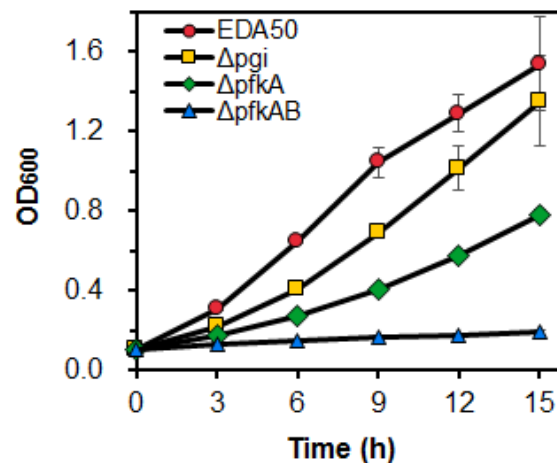
Figure 2. Cell growth of mutants with partial or complete disruption of the EMP with glucose as sole carbon source. OD_{600} profile of the unevolved(▲, Δ*pfkAB*) and evolved (●, EDA50) *E. coli* strain with the complete EMP-disruption and strains with partial EMP-disruption at phosphofructokinase step (◆, Δ*pfkA*) or phosphoglucose isomerase step (■, Δ*pgi*). Cells were aerobically grown in shaking flasks with 0.5% glucose M9 minimal media. Error bars indicates standard deviations of three independent biological replicates.

3.2 Identification of key genotype changes in the evolved mutant

Genome of EDA50 was sequenced and compared with the parental strain. Five mutations were detected in EDA50 (Table 1).

Table 3. Mutations acquired by EDA50 during adaptive evolution.

Gene	Gene product	Class	Nucleotide		Protein	
			Mutation (position)	Codon	Size(a.a)	Change
gntR	gluconate repressor protein	regulator	C422A (3577731)	GCG>GAG	331	A141E
galR	galactose repressor protein	regulator	G812A 2976599)	GGC>GAC	343	G271D
crp	cAMP response protein	regulator	G253T (3486120)	GCA>TCA	210	A85S
talB	transaldolase B	metabolic	C740T (8238)	GCA>GTA	317	A247V
ugd-	UDP-glucose 6-dehydrogenase	metabolic	Δ2312bp (2099438..)	-	388	-
gnd-	6-phosphogluconate dehydrogenase	metabolic			468	
wbbL-2	interrupted rhamnosyltransferase	-			-	

When isolating EDA50, four other evolved mutants exhibiting comparable growth with EDA50 were isolated together and denoted as EDA50-2, 3, 4, and 5, respectively (Fig. 3b). To estimate occurrence frequencies of each mutation, their existence in other isolates was analyzed. Mutations in *gntR*, *galR* and *ugd-gnd-wbbL-2* were detected in all EDA50 isolates while *crp* and *talB* mutations were detected only in one or two isolates (Fig. 3a). Then, in order to assess how significant each mutation contributes to improving fitness of EDA50 five mutants each carrying single mutation restoration were constructed and their fitness was compared with that of the original evolved mutant. Among five mutations, repairing each of three mutations in *gntR*, *galR* and *ugd-gnd-wbbL-2* displayed noticeable impact on growth of the evolved mutant. The EDA50_n, EDA50_l and EDA50_u each carrying single restoration of *gntR*, *galR* and *ugd-gnd-wbbL-2* mutation decreased 1.8-, 1.4-, and 1.3-fold decreased growth rate compared to EDA50, respectively. In contrast, repair of either *crp* and *talB* gene had minor and no effect (Fig. 3c). Both mutation frequency and repair analysis suggest that among identified mutations those in *gntR*, *galR* and *ugd-gnd-wbbL-2* would likely be responsible for enhanced cell growth with glucose as sole carbon source. To confirm that introduction of part or all three mutations can reproduce the growth phenotype of EDA50, the unevolved mutants with introduction of single or combination of those three candidates were constructed and their growth were compared with that of the original unevolved and the evolved mutant. The synergistic effect of those mutations on promoting cell growth of unevolved mutant was noticeable. When each of three mutations was introduced alone cell growth of resulting mutants was far below that of evolved mutant. The single *ugd-gnd-wbbL-2* deletion introduced mutant, AB_u, showed even lower cell growth than

the original mutant possibly due to loss of major glycolytic step. Both *gntR* and *galR* mutation introduced mutant, AB_n and AB_l, resulted in 2-fold increase in growth rate which corresponds to only 33% of that of evolved mutant. In contrast, AB_nlu possessing all those three mutations exhibited growth rate recovered up to 83% of that of EDA50 (Fig. 3d). Enhanced growth differentiating EDA50 from the unevolved mutant was attributed to occurrence of key mutations in *gntR*, *galR* and *ugd-gnd-wbbL-2* but also their synergetic encounter.
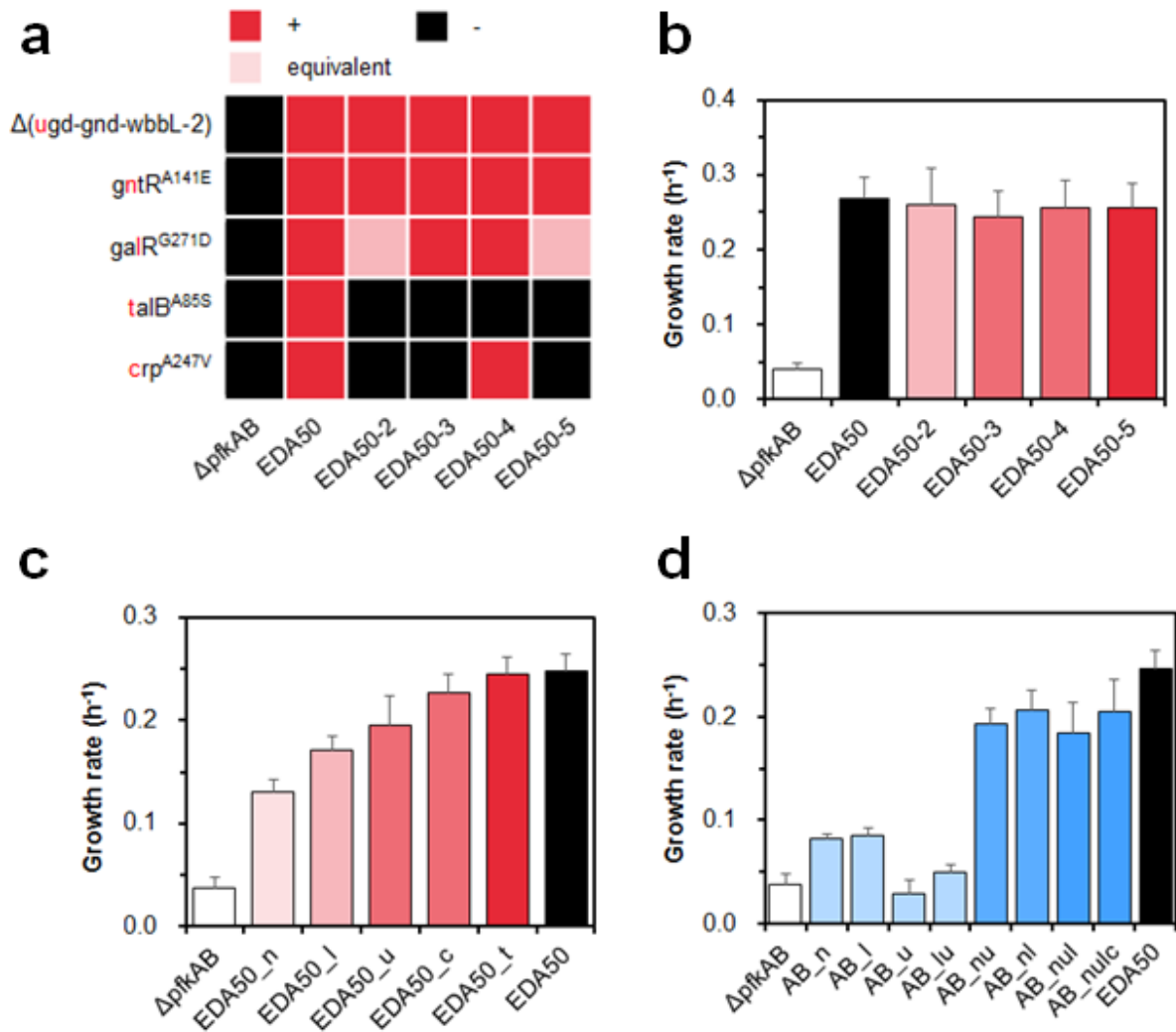
Figure 3. Identification of key genotype changes in EDA50. (a) The frequencies of mutations and (b) growth rate of the original and 5 evolved Δ*pfkAB* strains. (c) Effect of repairing each mutation in EDA50 on its growth rate. (d) Effect of introducing mutations discovered in the EDA50 to the unevolved strain with single or combinatorial manner. Cells were aerobically grown in shaking flasks with 0.5% glucose M9 minimal media. Error bars indicates standard deviations of three independent biological replicates.

3.3 Verification of real influential enzymes associated with key mutations.

In fact two key mutations in *gntR* and *galR* gene can affect expression of dozens of protein products because they encode transcription factors. Their positive effect on fitness observed the repair and reconstruction experiment might come from second-hand expression changes of such proteins rather from transcription factor itself. We tried to figure out expression change of which genes actually play for the phenotype change of the evolved mutant.

GntR represses expression of gluconate utilizing machinery when proper substrate feed is absent [37]. It also controls key genes of the ED pathway, *edd* and *eda*. It is because gluconate is converted into 6PG then metabolized *via* the ED pathway to give G3P and PYR (Fig. 4a). In EDA50, glucose metabolisms *via* the EMP and PP pathway were blocked due to absence of *pfkA*, *pfkB* and *gnd* gene (Table 1). It was reported that the *edd* and *eda* gene were expressed without gluconate by knocking-out *gntR* gene [38]. Therefore, we hypothesized that loss-of-function mutation in *gntR* gene renders the originally latent genes of the ED pathway de-repressed providing alternative route for glucose metabolism in EDA50.

E. coli mainly uptakes external glucose through PEP-dependent phosphotransferase system (PTS), which consists of enzyme I, HPr and glucose-specific EII complexes [39]. Upon disruption at upper glycolysis such as *pfkA* or *pgi ptsG* mRNAs stability is lowered and consequently PtsG expression level is decreased [19]. PtsG protein is a membrane receptor components of glucose-specific EII transporter complex of PTS [39]. Loss of PtsG resulted in retarded cell growth and slow glucose uptake rate due to limited capacity of glucose import [40]. Non-PTS glucose transporter such as GalP recovered glucose uptake rate in ptsG null mutant [40]. We expected that PtsG activity of the unevolved mutant is low due to destabilization of *ptsG* transcripts. GalR is a regulator which down-regulates genes for galactose metabolism when galactose is not available [41]. Regulon of GalR includes *galP* gene encoding galactose permease, which also shows activity to glucose [42]. Based on this we made a hypothesis that derepression of GalP gene due to mutated *galR* inactivating its product serves glucose transport instead of PtsG in EDA50 (Fig. 4b).

To prove our hypothesis, first we deleted mutant *gntR* and *galR* gene in EDA50 and denoted it as EDA50_Δn and EDA50_Δl, respectively. Deletion of *gntR* or *galR* gene had no effect on growth of EDA50 while restoration of these mutations resulted in notable negative effect on fitness of EDA50 (Fig. 4c). This result implies that even when their inducers are unavailable mutant GntR and GalR are unable to bind their target site and genes in their regulons are expressed. Then we expressed endogenous *edd-eda* and *galP* gene in *gntR*- and *galR*-repaired EDA50, respectively. As expected, expression of *edd-eda* and *galP* genes can functionally replace *gntR* and *galR* mutation in EDA50 showing they increased growth up to 90% and 100% of EDA50, respectively (Fig. 4c).

Other key mutation of large deletion covers two structural genes *ugd* and *gnd*. In order to verify true contributor for promoting fitness of EDA50, we deleted either of genes in EDA50_u which is EDA50 strain with deleted region of *ugd-gnd-wbbL-2* restored. Deletion of *gnd* gene in EDA50_u alone almost completely alleviated growth defect caused by loss of *ugd-gnd-wbbL-2* mutation (Fig. 4c).

Together with loss of Gnd activity, binding failure of mutant GntR and GalR to their target site de-repressed their regulons and among a number of regulated genes increase in expression of *edd-eda* and *galP* gene actually functions to facilitate growth of phosphofructokinase-deficient mutant. It is notable that two mutated genes *edd-eda* and *gnd* lie at 6PG node (Fig. 1). Interestingly, although both can support for alternative glycolysis complementing the interrupted EMP pathway early results showed that impacts of their expression on growth of EDA50 are in contrast: loss of *gnd* and gain of *edd-eda* expression for well-being. We investigated on how and what differentiates them regarding carrying out glucose catabolism.
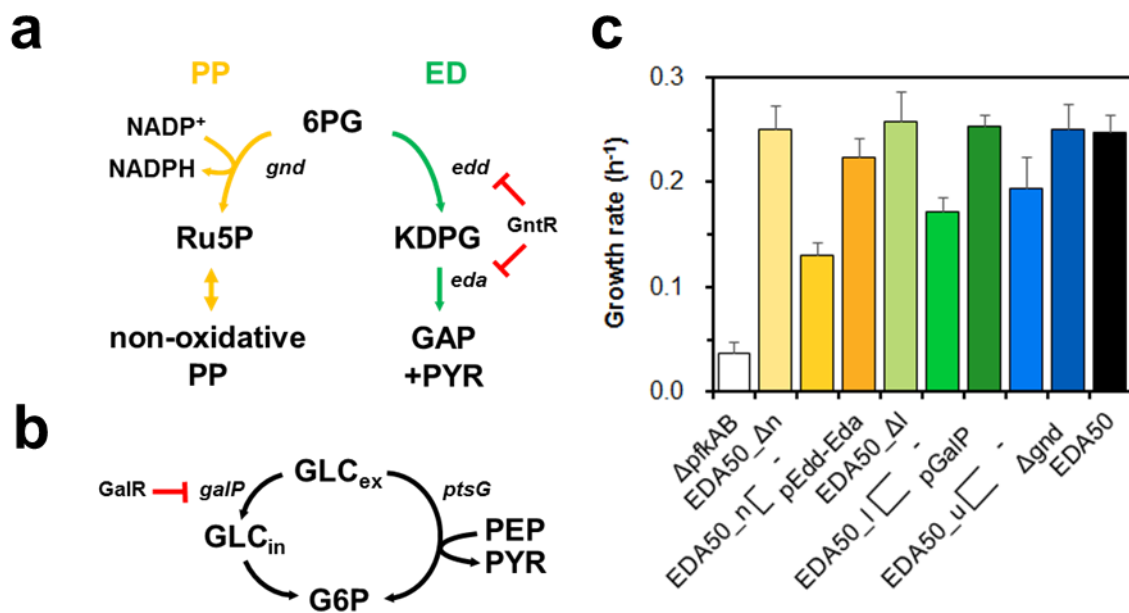
Figure 4. Figuring out true contributing proteins among proteins related with key genotype changes. (a) Description of *gnd* as a key gene of the oxidative PP pathway and GntR regulating key genes of the ED pathway, *edd-eda*. (b) Decription of major glucose import through phosphoenolpyruvate:phosphotransferase system (PTS) and GalR regulating PTS-independent glucose transport via glucose mease encoded by *galP*. (c) Growth rate of EDA50 with single mutation repair and corresponding compensation. Cells were aerobically grown in shaking flasks with 0.5% glucose M9 minimal media. 6.25 µM of IPTG was added at the beginning of both subculture and culture to induce each plasmid. Error bars indicates standard deviations of three independent biological replicates.

3.4 Opposing effect of activating the ED and PP pathway on fitness and redox regeneration.

We traced back how the operation of the PP and ED pathway affects physiology of the evolved mutant. While the 50th-day isolated evolved mutant employs only the ED pathway for glycolysis, the PP as well as ED pathway became available for catabolizing glucose in EDA50 carrying pGnd (Fig. 5a, b). When EDA50 harboring pGnd-GntR, its glycolysis mostly would rely on the PP pathway (Fig. 5a, c).
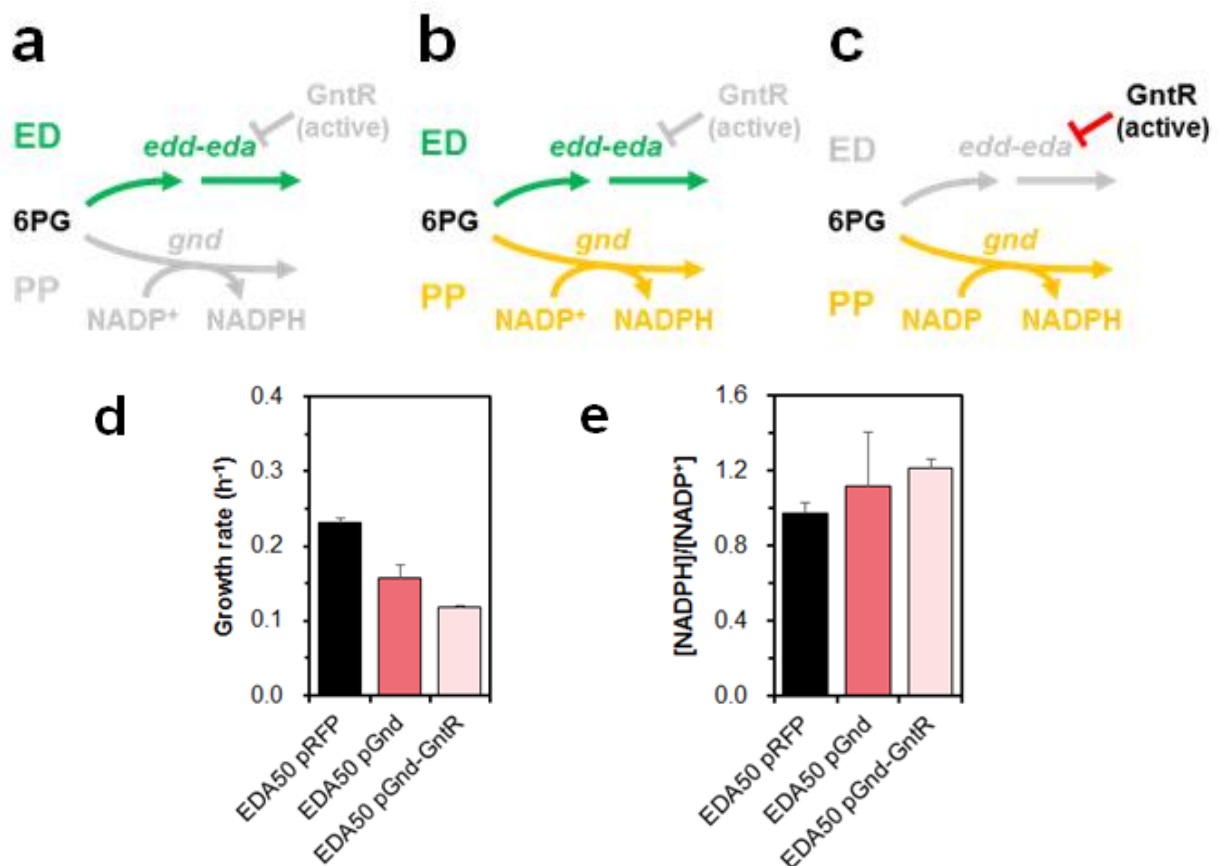
Figure 5. Effect of restoring the PP pathway and further inactivating the ED pathway. Decription of avilable glycolytic routes in (a) EDA50 pRFP, (b) EDA50 pGnd and (c) EDA50 pGnd-GntR strain. Effect of redirecting glycolytic flux from the ED pathway to the PP pathway in the evolved EDA50 strain on (d) growth rate and (e) [NADPH]/[NADP$^+$] ratio. Cells were aerobically grown in shaking flasks with 0.5% glucose M9 minimal media. 50 µM of IPTG was induced at 3-hour cultivation to induce each plasmid. The intracellular NADP(H) concentration was estimated 3-hour after induction. Error bars indicates standard deviations of three independent biological replicates.

We first investigated the effect of availability of the ED and the PP pathway on the fitness of EDA50. Enabling operation of the PP pathway had an adverse effect on cell growth of EDA50 both in the presence and absence of the ED pathway. Expression of Gnd in EDA50 led to 1.55-fold decrease in growth rate of EDA50. Further blockage of the ED pathway resulted in more severe growth defect resulting 1.95-fold reduction in cell growth compared to red fluorescence protein expressing EDA50 (Fig. 3c   and Fig. 5d).

In addition, consequences of 6PG metabolized through the ED or the PP pathway are apparently different in terms of NADPH regeneration. The conversion *via* the key enzyme of the PP pathway results in one NADPH regeneration while that *via* the key enzymes of ED pathway doesn't. (Fig. 5a-c) Therefore, the intracellular redox availability would be likely to depend on structure of the glycolytic pathways. To see this, [NADPH]/[NADP$^+$] ratios of EDA50 mutants with different glycolytic pathway structures were estimated. Recovering the PP pathway and additional suppressing the ED pathway increased [NADPH]/[NADP$^+$] ratio compared to when exclusively relying on the ED pathway. The [NADPH]/[NADP$^+$] ratio of EDA50 pGnd and EDA50 pGnd-GntR were 1.15- and 1.25-fold higher than that of EDA50 pRFP, respectively (Fig. 5e).

3.5 Rebalancing the ED and PP pathway for biotechnology application.

Microbial production of value-added chemicals often requires supply of reducing powers in the form of NADPH. Studies on metabolic production of chemicals showed that the production performances were often confined by insufficient NADPH availability [43]. Therefore, improving NADPH availability is desirable for enhanced productivity and yield of such chemicals [43]. That is, the optimal architectures of core metabolism to sustain normal growth and metabolic over-production are not alike. For successful employment of the evolved mutant to biorefinery, redesign of the metabolic core would be required. For proof of this concept, we introduced machineries for 3-hydroxypropionic acid (3-HP) production to the evolved mutant, EDA50. 3-HP is a platform chemical whose bi-functionality allows it to be further transformed into a variety of high value compounds [44]. From 1 mol of glucose 2 mol of 3-HP can be theoretically produced with consumption of 4 mol of NADPH (Fig. 6a). Its redox equivalent demand is far beyond endogenous catabolic supply considering glucose catabolism *via* the EMP pathway or the linear PP pathway regenerates 1 or 2 mol of NADPH per mol of glucose [12]. According to stoichiometry of the ED and cyclic PP pathway restoration of the cyclic PP and blockage of the ED pathway might give better 3-HP production result [15]. The permanent obstruction of the ED pathway, however, was unsuccessful to increase co-production of hydrogen and ethanol slowing down cell growth [23]. To address this issue, we demonstrate conditional flux control toward the ED and PP pathway at 6PG node for improved production of 3-HP.

Before dealing with redox issue we tried eliminating a limiting factor due to low malonyl-CoA

availability. Efficient microbial productions of chemicals using malonyl-CoA as precursor such as flavonoids and fatty acids were often confined by low its intracellular concentration [45]. Here, acetyl-CoA carboxylase (ACC) was overexpressed to increase its supply while site-directed mutation rendering endogenous enoyl-[acyl-carrier-protein] reductase to be temperature-sensitive was introduced to reduce consumption by fatty acid synthesis [46] (Fig. 6a).
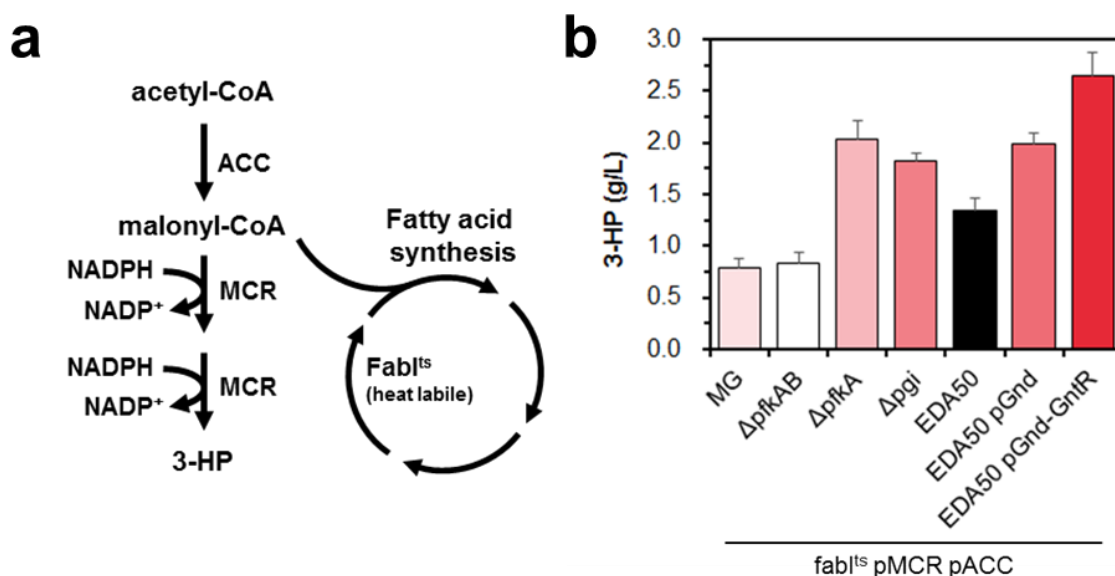
Figure 6. Rebalancing of the ED and PP pathway and 3-HP production. (a) Description of engineering for efficient production of 3-HP. Heterologous 3-HP synthetic pathway was introduce by expressing dissected form of malonyl-CoA reductase mutant originated from *C. aurantiacus*. For malonyl-CoA accumulation, ACC was overexpressed while fatty acid synthesis was reduced. (b) 3-HP production titer at 48-hour post-induction. 50 µM IPTG and 100 nM tetracycline were added 9-hour after culture start to induce plasmids. Error bars indicates standard deviations of three and two independent biological replicates

As expected, mere introduction of 3-HP producing machineries to the evolved mutant didn't result in significant improvement of production compared to the unevolved mutant. At 48-hour post induction, the unmodified EDA50-based strain produced 1.34 g/L of 3-HP while the unevolved-based one produced 0.83 g/L of 3-HP. Although the adapted mutant produced 1.6-fold higher 3-HP titer than the unevolved one when equipped equally, the fold-increase was subtle considering there was huge difference in biomass accumulation between them (Fig. 2 and Fig. 6b).

In order to achieve conditional flux rebalancing toward the ED and PP pathway, *E. coli gnd* and *gntR* genes are cloned under IPTG-inducible promoter and each resulting pGnd and pGnd-GntR plasmid was transformed to the 3-HP producing EDA50 mutant. The expression of each plasmid was delayed

so that the subsequent metabolic rearrangement didn't affect cell fitness significantly. Induction of flux redistribution to the ED and PP pathway led to considerable enhancement in 3-HP titer at 48-hour post-induction. The 3-HP producing EDA50 mutant harboring pGnd produced 1.99 g/L of 3-HP. Furthermore, when the ED pathway was repressed by additional expression of its down-regulator 2.65 g/L of 3-HP was produced from the evolved mutant, which is 3.2 times higher than that of the unevolved mutant furnished with the same 3-HP synthesis machinery (Fig. 6b). It indicates that not only the enabling glucose catabolism via the PP pathway but blockage of flux deviating to the ED pathway was important in enhancing 3-HP production.

IV. Discussion

In this work, we describe engineering of *E. coli* mutant employing alternative glycolytic routes with an aid of adaptive laboratory evolution to overcome metabolic sub-optimality upon glycolytic swap. We subjected the *E. coli* mutant without the EMP pathway to serial transfer in glucose minimal media. After the evolved mutant was isolated, reverse and forward engineering based on whole-genome sequencing identified key genotype changes alleviating metabolic obstacles hampering use of alternative glycolysis. Focusing on opposing direction of evolution for two alternative glycolytic pathways, the effect of varying their activity on physiology of the evolved mutant and 3-HP production availability was analyzed.

Glycolytic swap accompanies extensive changes in energy and redox status as well as availability of glycolytic intermediates including key signal molecules [47]. Such complexity hampers rational approaches to resolve metabolic sub-optimality by requiring simultaneous and cumulative activity change of multiple proteins rather single protein. Here, in *E. coli* we discovered synergetic role of enabling *galP* and *edd-eda* expression and deletion of *gnd* gene for well-functioning *E. coli* mutant without the functional EMP pathway from analysis of the adapted mutant. It is expected that there are two metabolic bottlenecks in mutant which lacks of phosphofructokinase: inability to import glucose and use of the sole PP pathway for glucose catabolism. Thus, concurrent enabling of brining in glucose with its catabolism by providing both alternative glucose transporter and catabolic pathway are essential to alleviate them.

Dating back to the middle of adaptive evolution, there must have been period when the PP and ED pathway coexisted because to possess of at least one glycolytic route loss of the PP pathway must have not occurred until awakening of the latent ED pathway. Then, why did the PP pathway have to vanish instead of to remain for serving glycolytic flux together with the ED pathway? It was suggested that one of the reasons the *E. coli pgi* knock-out mutant relying solely on the PP pathway for glucose catabolism showed reduced glucose uptake rate was due to inability to oxidize excess NADPH regenerated from the PP pathway [48]. When metabolized *via* the ED pathway one less NADPH is regenerated than *via* the PP pathway in this mutant [49]. Compared to *pgi* null mutant, the PP pathway of *pfkAB* knock-out mutant is able to regenerate NADPH even more intensively due to its cyclized architecture [15] (Fig. 1a). Considering this, impact of dragging flux to the ED pathway on reduction of regeneration of NADPH would be more significant in the later mutant. Despite of partial relief by the ED pathway the regeneration of NADPH *via* the cyclized PP pathway exceeds oxidation rate during normal growth. Excessive NADPH can mediate flux changes of NADPH-producing reactions [50]. Especially, in $\Delta pfkAB$ strain the glucose 6-phosphate dehydrogenase (G6PDH) is essential for glucose metabolism. *E. coli* G6PDH is subjected to allosteric regulation by NADPH [51].

Therefore, overall glycolytic rate can be retarded by high [NADPH]/[NADP$^+$] ratio. In addition, the ED pathway is thermodynamically more feasible even than native glycolytic route, the EMP pathway, is [8, 13]. The thermodynamic favorable property enables the ED pathway to sustain the equivalent glycolytic flux to the EMP pathway with several folds-less amount of enzymes [8, 13]. In fact, *Z. mobilis* employing the ED pathway for glycolysis uptakes glucose remarkably fast [14]. This reflects that the capacity and turnover rate of the ED pathway would be substantial as it is called catabolic highway [52, 53]. Considering all, rendering the ED pathway to become sole glycolytic route rather to share flux with the PP pathway would benefit the phosphofructokinase deficient mutant in term of both reducing NADPH and expanding glycolytic capacity during selection.

Although the metabolic transition from the PP to ED pathway partially alleviated extreme NADPH regeneration from the cyclized PP pathway, glycolysis via the sole ED pathway also produces one more NADPH compared to that of the EMP pathway [12]. Indeed, several native strains adopting the ED or PP pathway share loose cofactor specificity of oxidoreductases as strategy to avoid overproduction of NADPH [10]. Especially, G6PDHs from such strains exhibit subsequent activity with NAD$^+$ compared to that from *E. coli* which is strictly NADP$^+$-specific [10, 54-56]. Introducing NAD$^+$-dependent G6PDH and controlling its activity in response to anabolic NADPH demand would meet different requirement of NADPH during growth and bio-synthesis phase.

It was suggested that in the Δ*pfkA*B strain the glucose transport has been unable due to post-transcriptional inhibition of major glucose transport *via* PTS [19]. Although PTS-independent glucose transporter enabled glucose import, the loss of PtsG protein would complicate the physiology of the EMP-disrupted strains due to large-scale change in transcriptome. Absence of PtsG activates adenylcyclase and cAMP level would be abnormally increased when glucose is available [57]. Mediated by cAMP-binding protein CRP affecting transcription of over 400 genes, the global gene expression pattern would be totally changed [58]. Such complexity could be resolved by restoring the expression of PtsG by removing of regulatory RNA binding site in 5'-UTR region of *ptsG* gene [59]. In the meanwhile, another possible reason for reduced capacity of glucose uptake in the EMP-disrupted strains could be low availability of PEP which is essential for PTS-dependent glucose uptake. Previous studies showed that the Δ*pfkA* mutant has reduced PEP concentration [16]. In addition, increase in flux through the ED pathway can further lower intracellular PEP pool [18]. It is supported by the stoichiometry the ED pathway where PEP generation per glucose is half of that of the PP or EMP pathway [12]. Limited glucose importing capacity due to low PEP availability can be redeemed by expression PEP-independent glucose permease and if necessary, glucose kinase [40]. Considering all, in order to enable glucose transport with side effects minimized it is highly recommended to restore the disabled glucose PTS and to supplement limited capacity by expressing PEP-independent glucose transport machineries.

V. Conclusion

This study describes physiology and engineering of *E. coli* strain utilizing alternative form of glycolysis. From genotype-phenotype relationship of the evolved strain, it was suggested that the simultaneous enabling of glucose import and glycolytic transition from the PP to ED pathway was critical in mitigating arrested growth of strain deficient of the functional EMP pathway. In addition, the divergent role of the ED and PP pathway in fitness and NADPH regeneration capacity was addressed. Focusing on trade-off between fitness and NADPH regeneration while activating the ED pathway, the conditional rebalancing of the ED and PP pathway was introduced to adjust NADPH regeneration capacity without sacrificing cell growth. Finally, based on the results presented here and several related report in literature, strategies for further refinement were discussed.

References

1. Müller M, Mentel M, van Hellemond JJ, Henze K, Woehle C, Gould SB, Yu R-Y, van der Giezen M, Tielens AGM, Martin WF: Biochemistry and Evolution of Anaerobic Energy Metabolism in Eukaryotes. *Microbiology and Molecular Biology Reviews* 2012, 76:444-495.

2. Sato T, Atomi H: Novel metabolic pathways in Archaea. *Current Opinion in Microbiology* 2011, 14:307-314.

3. Fraenkel DG, Vinopal RT: Carbohydrate Metabolism in Bacteria. *Annual Review of Microbiology* 1973, 27:69-100.

4. Bar-Even A, Flamholz A, Noor E, Milo R: Rethinking glycolysis: on the biochemical logic of metabolic pathways. *Nature Chemical Biology* 2012, 8:509.

5. Toya Y, Ishii N, Nakahigashi K, Hirasawa T, Soga T, Tomita M, Shimizu K: 13C-metabolic flux analysis for batch culture of Escherichia coli and its pyk and pgi gene knockout mutants based on mass isotopomer distribution of intracellular metabolites. *Biotechnology Progress* 2010, 26:975-992.

6. Halevas EG, Pantazaki AA: Advances in the optimized synthesis of biotechnologically valuable products from bioengineered microbial cell factories. *Biointerface Research in Applied Chemistry* 2018, 8:3463-3482.

7. Aslan S, Noor E, Bar-Even A: Holistic bioengineering: rewiring central metabolism for enhanced bioproduction. *Biochemical Journal* 2017, 474:3935-3950.

8. Flamholz A, Noor E, Bar-Even A, Liebermeister W, Milo R: Glycolytic strategy as a tradeoff between energy yield and protein cost. *Proceedings of the National Academy of Sciences* 2013, 110:10039-10044.

9. Reznik E, Christodoulou D, Goldford JE, Briars E, Sauer U, Segrè D, Noor E: Genome-Scale Architecture of Small Molecule Regulatory Networks and the Fundamental Trade-Off between Regulation and Enzymatic Activity. *Cell Reports* 2017, 20:2666-2677.

10. Fuhrer T, Sauer U: Different Biochemical Mechanisms Ensure Network-Wide Balancing of Reducing Equivalents in Microbial Metabolism. *Journal of Bacteriology* 2009, 191:2112-2121.

11. Chen X, Schreiber K, Appel J, Makowka A, Fähnrich B, Roettger M, Hajirezaei MR, Sönnichsen FD, Schönheit P, Martin WF, Gutekunst K: The Entner–Doudoroff pathway is an overlooked glycolytic route in cyanobacteria and plants. *Proceedings of the National Academy of Sciences* 2016, 113:5441-5446.

12. Liu H, Sun Y, Ramos KRM, Nisola GM, Valdehuesa KNG, Lee WK, Park SJ, Chung W-J:

Combination of Entner-Doudoroff Pathway with MEP Increases Isoprene Production in Engineered Escherichia coli. *PLOS ONE* 2013, 8:e83290.

13. Abernathy MH, Zhang Y, Hollinshead WD, Wang G, Baidoo EEK, Liu T, Tang YJ: Comparative studies of glycolytic pathways and channeling under in vitro and in vivo modes. *AIChE Journal* 2019, 65:483-490.

14. Fuhrer T, Fischer E, Sauer U: Experimental Identification and Quantification of Glucose Metabolism in Seven Bacterial Species. *Journal of Bacteriology* 2005, 187:1581-1590.

15. Kruger NJ, von Schaewen A: The oxidative pentose phosphate pathway: structure and organisation. *Current Opinion in Plant Biology* 2003, 6:236-246.

16. Siedler S, Bringer S, Blank LM, Bott M: Engineering yield and rate of reductive biotransformation in Escherichia coli by partial cyclization of the pentose phosphate pathway and PTS-independent glucose transport. *Applied microbiology and biotechnology* 2012, 93:1459-1467.

17. Siedler S, Bringer S, Polen T, Bott M: NADPH-dependent reductive biotransformation with Escherichia coli and its pfkA deletion mutant: Influence on global gene expression and role of oxygen supply. *Biotechnology and Bioengineering* 2014, 111:2067-2075.

18. Hollinshead WD, Rodriguez S, Martin HG, Wang G, Baidoo EEK, Sale KL, Keasling JD, Mukhopadhyay A, Tang YJ: Examining Escherichia coli glycolytic pathways, catabolite repression, and metabolite channeling using Δpfk mutants. *Biotechnology for Biofuels* 2016, 9:212.

19. Morita T, El-Kazzaz W, Tanaka Y, Inada T, Aiba H: Accumulation of glucose 6-phosphate or fructose 6-phosphate is responsible for destabilization of glucose transporter mRNA in Escherichia coli. *J Biol Chem* 2003, 278:15608-15614.

20. Li C, Ying L-Q, Zhang S-S, Chen N, Liu W-F, Tao Y: Modification of targets related to the Entner–Doudoroff/pentose phosphate pathway route for methyl-d-erythritol 4-phosphate-dependent carotenoid biosynthesis in Escherichia coli. *Microbial Cell Factories* 2015, 14:117.

21. Dragosits M, Mattanovich D: Adaptive laboratory evolution – principles and applications for biotechnology. *Microbial Cell Factories* 2013, 12:64.

22. Fong SS, Nanchen A, Palsson BO, Sauer U: Latent pathway activation and increased pathway capacity enable Escherichia coli adaptation to loss of key metabolic enzymes. *J Biol Chem* 2006, 281:8024-8033.

23. Sundara Sekar B, Seol E, Mohan Raj S, Park S: Co-production of hydrogen and ethanol by pfkA-deficient Escherichia coli with activated pentose-phosphate pathway: reduction of pyruvate accumulation. *Biotechnology for Biofuels* 2016, 9:95.

25. Kim CH: An engineered E. coli with EDP enhancement, PPP cyclization and FadR

overexpression to increase medium chain fatty acid synthesis. Ulsan National Institute of Science and Technology, Department of Biomedical Engineering; 2018.

35. Kim SM, Choi BY, Ryu YS, Jung SH, Park JM, Kim G-H, Lee SK: Simultaneous utilization of glucose and xylose via novel mechanisms in engineered Escherichia coli. *Metabolic Engineering* 2015, 30:141-148.

36. Hellinga HW, Evans PR: Nucleotide sequence and high-level expression of the major Escherichia coli phosphofructokinase. *European Journal of Biochemistry* 1985, 149:363-373.

37. Peekhaus N, Conway T: What's for dinner?: Entner-Doudoroff metabolism inEscherichia coli. *Journal of bacteriology* 1998, 180:3495-3502.

38. Nagai H, Masuda A, Toya Y, Matsuda F, Shimizu H: Metabolic engineering of mevalonate-producing Escherichia coli strains based on thermodynamic analysis. *Metabolic Engineering* 2018, 47:1-9.

39. Postma PW, Lengeler JW: Phosphoenolpyruvate:carbohydrate phosphotransferase system of bacteria. *Microbiological reviews* 1985, 49:232-269.

40. Lu J, Tang J, Liu Y, Zhu X, Zhang T, Zhang X: Combinatorial modulation of galP and glk gene expression for improved alternative glucose utilization. *Appl Microbiol Biotechnol* 2012, 93:2455-2462.

41. Weickert MJ, Adhya S: The galactose regulon of Escherichia coli. *Mol Microbiol* 1993, 10:245-251.

42. Geanacopoulos M, Adhya S: Functional characterization of roles of GalR and GalS as regulators of the gal regulon. *Journal of bacteriology* 1997, 179:228-234.

43. Wang Y, San K-Y, Bennett GN: Cofactor engineering for advancing chemical biotechnology. *Current Opinion in Biotechnology* 2013, 24:994-999.

44. Kumar V, Ashok S, Park S: Recent advances in biological production of 3-hydroxypropionic acid. *Biotechnology Advances* 2013, 31:945-961.

45. Zha W, Rubin-Pitel SB, Shao Z, Zhao H: Improving cellular malonyl-CoA level in Escherichia coli via metabolic engineering. *Metabolic Engineering* 2009, 11:192-198.

47. Persson Ö, Valadi Å, Nyström T, Farewell A: Metabolic control of the Escherichia coli universal stress protein response through fructose-6-phosphate. *Molecular Microbiology* 2007, 65:968-978.

48. Canonaco F, Hess TA, Heri S, Wang T, Szyperski T, Sauer U: Metabolic flux response to phosphoglucose isomerase knock-out in Escherichia coli and impact of overexpression of the soluble transhydrogenase UdhA. *FEMS Microbiology Letters* 2001, 204:247-252.

49. Fischer E, Sauer U: Metabolic flux profiling of Escherichia coli mutants in central carbon metabolism using GC-MS. *European Journal of Biochemistry* 2003, 270:880-891.

50.   Bautista J, Satrústegui J, Machado A: Evidence suggesting that the NADPH/NADP ratio modulates the splitting of the isocitrate flux between the glyoxylic and tricarboxylic acid cycles, in Escherichia coli. *FEBS Letters* 1979, 105:333-336.

51.   Banerjee S, Fraenkel DG: Glucose-6-phosphate dehydrogenase from Escherichia coli and from a "high-level" mutant. *Journal of bacteriology* 1972, 110:155-160.

52.   Sprenger GA: Carbohydrate metabolism in Zymomonas mobilis: a catabolic highway with some scenic routes. *FEMS Microbiology Letters* 1996, 145:301-307.

53.   Ng CY, Farasat I, Maranas CD, Salis HM: Rational design of a synthetic Entner–Doudoroff pathway for improved and controllable NADPH regeneration. *Metabolic Engineering* 2015, 29:86-96.

54.   Olavarria K, Marone MP, da Costa Oliveira H, Roncallo JC, da Costa Vasconcelos FN, da Silva LF, Gomez JGC: Quantifying NAD(P)H production in the upper Entner-Doudoroff pathway from Pseudomonas putida KT2440. *FEBS open bio* 2015, 5:908-915.

55.   Pentjuss A, Odzina I, Kostromins A, Fell DA, Stalidzans E, Kalnenieks U: Biotechnological potential of respiring Zymomonas mobilis: A stoichiometric analysis of its central metabolism. *Journal of Biotechnology* 2013, 165:1-10.

56.   Olavarria K, De Ingeniis J, Zielinski DC, Fuentealba M, Munoz R, McCloskey D, Feist AM, Cabrera R: Metabolic impact of an NADH-producing glucose-6-phosphate dehydrogenase in Escherichia coli. *Microbiology* 2014, 160:2780-2793.

57.   Steinsiek S, Bettenbrock K: Glucose transport in Escherichia coli mutant strains with defects in sugar transport systems. *Journal of bacteriology* 2012, 194:5897-5908.

58.   Gosset G, Zhang Z, Nayyar S, Cuevas WA, Saier MH, Jr.: Transcriptome analysis of Crp-dependent catabolite control of gene expression in Escherichia coli. *Journal of bacteriology* 2004, 186:3516-3524.

59.   Rice JB, Vanderpool CK: The small RNA SgrS controls sugar-phosphate accumulation by regulating multiple PTS genes. *Nucleic acids research* 2011, 39:3806-3819.

24.   Blattner FR, Plunkett G, 3rd, Bloch CA, Perna NT, Burland V, Riley M, Collado-Vides J, Glasner JD, Rode CK, Mayhew GF, et al: The complete genome sequence of Escherichia coli K-12. *Science* 1997, 277:1453-1462.

26.   Ryu YS, Chandran S-P, Kim K, Lee SK: Oligo- and dsDNA-mediated genome editing using a tetA dual selection system in Escherichia coli. *PLOS ONE* 2017, 12:e0181501.

27.   Lee TS, Krupa RA, Zhang F, Hajimorad M, Holtz WJ, Prasad N, Lee SK, Keasling JD: BglBrick vectors and datasheets: A synthetic biology platform for gene expression. *Journal of biological engineering* 2011, 5:12-12.

28.   Datta S, Costantino N, Court DL: A set of recombineering plasmids for gram-negative

bacteria. *Gene* 2006, 379:109-115.

29.   Datsenko KA, Wanner BL: One-step inactivation of chromosomal genes in Escherichia coli K-12 using PCR products. *Proceedings of the National Academy of Sciences of the United States of America* 2000, 97:6640-6645.

30.   Cherepanov PP, Wackernagel W: Gene disruption in Escherichia coli: TcR and KmR cassettes with the option of Flp-catalyzed excision of the antibiotic-resistance determinant. *Gene* 1995, 158:9-14.

31.   Liu C, Ding Y, Zhang R, Liu H, Xian M, Zhao G: Functional balance between enzymes in malonyl-CoA pathway for 3-hydroxypropionate biosynthesis. *Metabolic Engineering* 2016, 34:104-111.

32.   Shin KS, Lee SK: Introduction of an acetyl-CoA carboxylation bypass into Escherichia coli for enhanced free fatty acid production. *Bioresource Technology* 2017, 245:1627-1633.

33.   Wong T-K, Neumann E: Electric field mediated gene transfer. *Biochemical and Biophysical Research Communications* 1982, 107:584-587.

34.   Rathnasingh C, Raj SM, Lee Y, Catherine C, Ashok S, Park S: Production of 3-hydroxypropionic acid via malonyl-CoA pathway using recombinant Escherichia coli strains. *Journal of Biotechnology* 2012, 157:633-640.

46.   Kleerebezem M, Heutink M, de Cock H, Tommassen J: The qmeA (ts) mutation of Escherichia coli is localized in the fabI gene, which encodes enoyl-ACP reductase. *Research in Microbiology* 1996, 147:609-613.

Acknowledgments